Mon. Not. R. astr. Soc. (1978) **185**, 527–538

A dynamical interpretation of the radio jet in 3C 31

R. D. Blandford and V. Icke *W. K. Kellogg Radiation Laboratory, California Institute of Technology, Pasadena, California 91125, USA*

Received 1978 May 3; in original form 1978 March 28

Summary. The radio source 3C 31, which is positionally identified with the galaxy NGC 383, has recently been shown to contain two curved radio jets emanating from the galaxy's nucleus. In this paper, we demonstrate that the projected shape of these jets may be produced by a dynamical interaction between NGC 383 and its neighbour NGC 382. On the basis of this hypothesis, the orbital elements of the NGC 383/NGC 382 system are estimated and a mean V magnitude mass to light ratio of about 11 solar units is derived for the system. The inferred value for the jet velocity is approximately 500 km/s. Some consequences for theoretical models of other extragalactic radio sources are briefly outlined.

1 Introduction

Several extragalactic radio sources have been shown to contain linear jets. Prominent examples include NGC 6251 (Waggett, Warner & Baldwin 1977), 3C 315 (Bridle *et al.* 1976) and 3C 219 (Turland 1975). The existence of these jets furnishes strong evidence for the view that mass, energy and momentum are continuously supplied to the radio lobes of all double sources through a supersonic beam emanating from the nucleus of an associated galaxy or quasar. This poses several interesting questions; in particular, what are the characteristic fluid velocities within the jets and what is the nature of the dynamical interaction of the jets with the surrounding medium?

Burch (1977) has recently published a set of multi-frequency, high-resolution maps of 3C 31. This object is a low-power ($\sim 10^{34}$ W) source associated with the bright elliptical galaxy NGC 383, which is the dominant member of the galaxy chain Arp 331 (Arp 1966). The most prominent feature of these maps is a pair of jets emerging in antiparallel directions from the nucleus of NGC 383, which both have several well-resolved sharp bends within a projected distance of about 100 kpc from the galaxy. The entire source extends over about 1 Mpc but only shows large-scale departures from linearity in the outermost regions.

Similar sharp bends are a common feature of radio trails (e.g. NGC 1265; Wellington, Miley & van der Laan 1973) and are convincingly explained in terms of a dynamical interaction with the surrounding medium caused by the relative motion of the parent galaxy. However, in the case of 3C 31, there is reason to believe that this is not the explanation.

Firstly, both jets initially bend towards the west, and then revert approximately to their original direction, the first bend occurring at a projected distance of about 25 kpc. It would be extremely surprising if the velocity field in the surrounding medium had structure on this small a scale and yet did not destroy the overall integrity of the source. Secondly, unlike nearly all radio trails, 3C 31 is not known to be in a rich cluster. As we discuss further in Section 4, the gas density in the surrounding medium is unlikely to be large enough to cause the observed distortion in the jet. We therefore propose that the nucleus of NGC 383 emits two antiparallel, linear jets which, to a first approximation, propagate ballistically away from the galaxy. The observed bends in the jet are attributed to the acceleration experienced by NGC 383 during dynamical interaction with other members of the small group. (That the closest bends in the northern and southern jets are in the same direction rules out the possibility that they may be attributed to changes in the direction of the emission axis of the nuclear source.) A qualitatively similar explanation has been proposed for the source 1200 + 519 by Miley & Harris (1977) and a quantitative model of the radio trail 3C 129 has been made by Byrd & Valtonen (1978). We note, however, that only *one* encounter suffices to produce a *double* bend in the trajectory of a jet.

Table 1. Data for NGC 383 and NGC 382 derived from Humason *et al.* (1956).

	NGC 383	NGC 382
radial velocity (km/s)	4888	5156
m_p [2]	13.6	15.3 [1]
$m_B - m_v$	1.0	1.0
M_V	−22.8	−21.1
$(M/L)_V$ [3]	11	13

Notes:

1. The quoted photographic magnitude for NGC 382 (m_p = 14.2) is apparently incorrect (see Plate 1). It has been replaced by a visual estimate.
2. We assume $m_p - m_B$ = 0.1 and 0.5 mag of visual extinction.
3. The mass to light ratio is expressed in terms of $M_\odot/L_{V\odot}$ and uses the masses given in Table 2.

At a projected distance of only 16 kpc from NGC 383 (adopting a distance of 100 Mpc for this galaxy) is located the elliptical galaxy NGC 382. The difference in radial velocity between these objects is 268 km/s (Humason, Mayall & Sandage 1956; our Table 1). The galaxies are included as a pair in Karachentsev's (1972) catalogue of binary galaxies. Unless NGC 382 lies almost on the line of sight to NGC 383, we cannot avoid the conclusion that the two galaxies are undergoing a close encounter. The motion of NGC 383 should then be reflected in the jet. We show below that it is possible to reproduce the observed shape of the inner ~200 kpc of both jets if we make the simplest assumption of a two-body encounter and ignore the influence of all the other galaxies in the group. From the derived orbit we can then obtain the masses of the galaxies, free from the uncertain projection factors that are present in conventional mass determinations using binary galaxies. We can also measure the velocity of the jet by this method and hence speculate upon the dynamics of such jets, inferred and observed in other double sources.

2 Dynamics of an orbiting jet

Consider a jet pointing along an inertially fixed direction in space, the source of which moves so that its position at time t is $\mathbf{R}(t)$. If the fluid in the jet moves uniformly away from

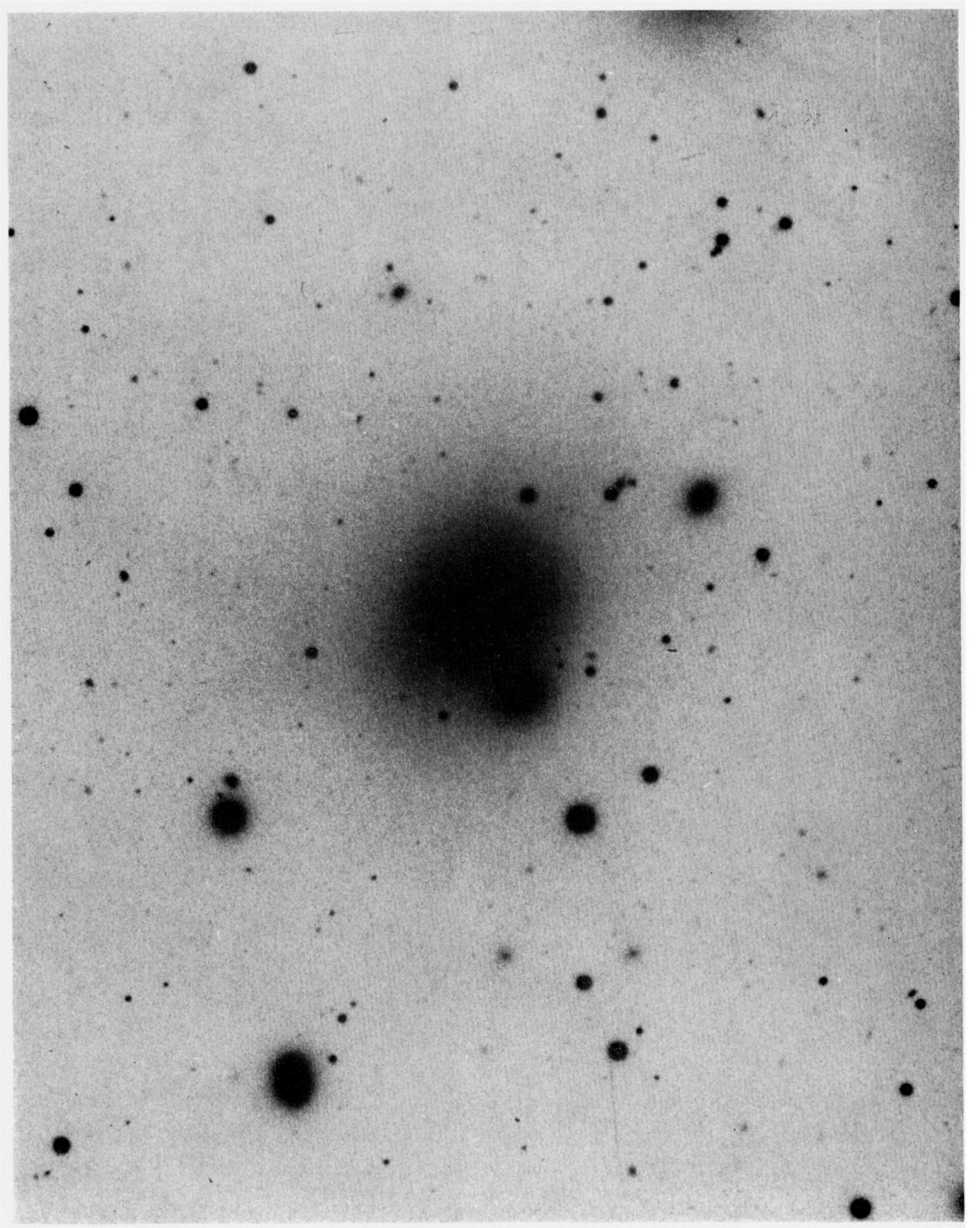

Plate 1. High-density print of the region around NGC 383 reproduced from a sky-limited red plate taken on the 4-m telescope at the Kitt Peak National Observatory by Dr H. C. Arp.

facing page 528]

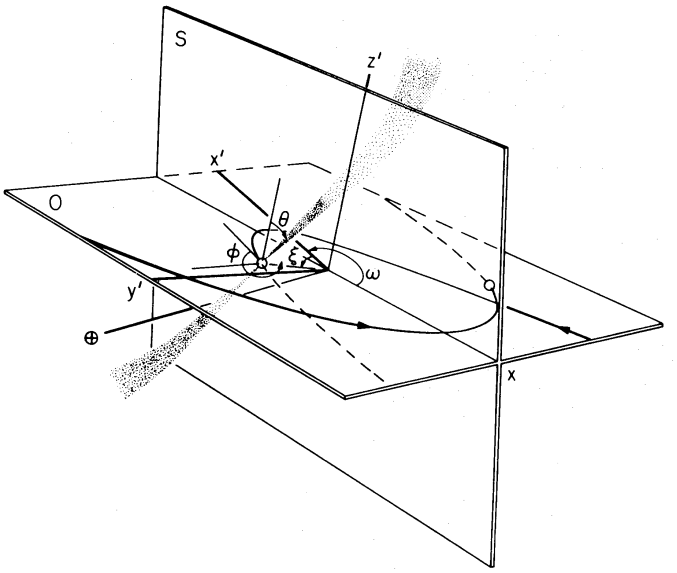

Figure 1. Representation of the galaxy and jet trajectories. S is the plane of the sky and O the orbital plane; x', y', z' are the coordinate axes of the orbit. The direction of the observer, designated ⊕, is the z axis.

the source with constant velocity **u**, the observed jet at time t' is given by

$$\mathbf{r}(t) = \mathbf{R}(t) - (t - t')\{\mathbf{u} + \dot{\mathbf{R}}(t)\}; t \leqslant t', \tag{1}$$

parametrized by t. (Note that if the source moves uniformly, a straight jet in the direction of **u** originating from the *present* source position $R(0)$ is observed.)

If we ignore projection effects, it is straightforward to show that the fact that the radius of curvature of the jet is comparable with the separation of the galaxies (see Fig. 2) implies that the effect of gravity on the motion of the jet cannot be ignored and that $u \sim \dot{R}$.

It is convenient to calculate the locus of the jet in orbital (primed) coordinates, with the origin at the centre of mass, the x' axis through the perigalacticon of NGC 383, the z' axis along the orbital angular momentum and the y' axis to form a right-handed triad (x', y', z') (Fig. 1). In addition, the subscript $i = 1$ will refer to NGC 383 and 2 to NGC 382. We assume that the two masses m_1 and m_2 follow a Keplerian orbit, but we use a softened Plummer potential with core radii c_i (corresponding to an $n = 5$ polytrope) in the computation of the force exerted on the jet:

$$\Phi_i = -Gm_i(|\mathbf{r}(t') - \mathbf{R}_i(t')|^2 + c_i^2)^{-1/2}. \tag{2}$$

We discuss the origin of this softening in Section 4 below.

If we measure lengths in units of p, the semi-latus rectum of the relative orbit, and times in units of $(p^3/Gm)^{1/2}$ where $m = m_1 + m_2$, then the total angular momentum per unit reduced mass is unity and the equations of motion for the jet, in terms of the true anomaly $\zeta(t)$ measured from perigalacticon, are given by

$$\frac{d\mathbf{r}'}{d\zeta'} = R'^2\mathbf{v}' \tag{3}$$

$$\frac{d\mathbf{v}'}{d\zeta'} = -(1-f)R'^2(\mathbf{r}' - f\mathbf{R}')(|\mathbf{r}' - f\mathbf{R}'|^2 + c_1^2)^{-3/2}$$
$$-fR'^2(\mathbf{r}' + (1-f)\mathbf{R}')(|\mathbf{r}' + (1-f)\mathbf{R}'|^2 + c_2^2)^{-3/2}$$

$$\zeta(t) \equiv \zeta \leqslant \zeta' \equiv \zeta(t') \leqslant \zeta_0 \equiv \zeta(0)$$

where $\mathbf{v}'$ is the jet velocity, $f = m_2/m$,

$$\mathbf{R}'(\zeta') = 1 + e\cos\zeta')^{-1}(\cos\zeta', \sin\zeta', 0)$$

$$\dot{\mathbf{R}}'(\zeta') = (-\sin\zeta', (\cos\zeta' + e), 0)$$

and the initial conditions are

$$\mathbf{r}'(\zeta) = f\mathbf{R}'(\zeta)$$

$$\mathbf{v}'(\zeta) = f\dot{\mathbf{R}}'(\zeta) + \mathbf{u}.$$

The jet velocity $\mathbf{u}$ is $u(\sin\theta\cos\phi, \sin\theta\sin\phi, \cos\theta)$ in the orbit coordinate system.

Equations (3), (4) are to be integrated from ζ to ζ_0 to give the position $r'(\zeta_0)$ of the jet at present, that is, $t = 0$. The vectors $\mathbf{R}'$, $\dot{\mathbf{R}}'$, $\mathbf{r}'$ are transformed into sky coordinates $\mathbf{R}$, $\dot{\mathbf{R}}$, $\mathbf{r} = (x, y, z)$ through the operation $\mathbf{R} = \mathbf{M}\mathbf{R}'$, etc., where the matrix $\mathbf{M}$ is

$$\mathbf{M} = \begin{pmatrix} \cos\omega & -\sin\omega & 0 \\ \sin\omega\cos i & \cos\omega & \cos\omega\sin i \\ -\sin\omega\sin i & -\cos\omega\sin i & \cos i \end{pmatrix}, \tag{5}$$

ω is the longitude of perigalacticon measured from the receding node and $i = \cos^{-1}(\mathbf{z}'\cdot\mathbf{z})$ is the inclination. The locus of the observed jet is then $\{x(\zeta), y(\zeta)\}$, parametrized by the true anomaly ζ of the source at the time when the element of jet was emitted.

From the present difference in radial velocities of the two galaxies $\Delta V = -(n.\dot{R}_0)(Gm/p)^{1/2}$ and their projected separation $d = p\{R_0^2 - (\mathbf{n}\cdot\mathbf{R}_0)^2\}^{1/2}$ (where n is the unit vector along the line of sight), we calculate the mass sum m using

$$m = (\Delta V)^2 \frac{d}{G}(\mathbf{n}\cdot\dot{\mathbf{R}}_0)^{-2}\{R_0^2 - (\mathbf{n}\cdot\mathbf{R}_0)^2\}^{-1/2}. \tag{6}$$

Implicit in this calculation of the mass are nine parameters that will be adjusted so as to obtain the best fit to the observed jet: f, u_N (the speed of the northern jet), u_S (the speed of the southern jet), θ, ϕ (spherical polar angles for the northern jet direction) ω, i, e, ζ_0. We can eliminate ζ_0 from these parameters by substituting the observed angle $\chi = 44°$ between the northern jet and the line of galaxies (see Fig. 1), using

$$\tan(\omega + \xi_0) = \left[\frac{\tan\chi\sec i + \tan(\phi+\omega) + \cot\theta\tan i\sec(\phi+\omega)}{1 - \tan\chi\{\cos i\tan(\phi+\omega) + \cot\theta\sin i\sec(\phi+\omega)\}}\right]. \tag{7}$$

This leaves eight independent parameters. In addition, as we discuss further below, the galactic core radii are also adjustable and can influence the shape of the jet.

3 Application to NGC 382/NGC 383

3.1 INITIAL GUESSED PARAMETERS

In Fig. 2 we see that the northern jet proceeds directly to A where it bends sharply westward, bending back approximately northward again at B. These bends correspond to more gentle curves in the southern jet at C and D. The simplest interpretation of these bends is that they are due to the large acceleration experienced by NGC 383 upon its passage through perigalacticon. The north–south asymmetry indicates that during this passage NGC 383 was moving approximately parallel to the projection of the northern jet onto the orbital plane.

As NGC 383 approaches us from the centre of mass, we guess that $\omega \sim 180°$ and $i \sim 100°$. The abrupt character of the bends in the northern jet indicates a fairly eccentric orbit, $e \sim 1$. In addition, there is a prominent bend in the southern jet at E. Whilst this may be caused by a superposed radio source, unassociated with the jet, a more attractive explanation is that it was produced prior to perigalacticon passage when the southern jet passed close to NGC 382. This indicates that $\theta \sim 60°$, $\phi \sim 270°$. We can complete the set of first guesses setting $u_N \sim u_S \sim 1$ as suggested in Section 1, and $f \sim 0.2$, weighting the galaxies in proportion to their approximate luminosities. (We have in fact carried out a search of the full eight-dimensional parameter space, and are reasonably convinced that a satisfactory fit to both jets can only be obtained using approximately these parameters.)

3.2 BEST-FITTING PARAMETERS

Equations (3) and (4) were integrated using a standard fourth-order Runge–Kutta scheme. The resultant jet loci were plotted for different sets of the eight parameters and the two core radii. These parameters were adjusted individually to produce a locus that appeared to reproduce most of the innermost parts of the observed jets. (An attempt was made to improve the accuracy of the fit by incorporating a least-squares fitting routine, but this was abandoned because it was found that the necessarily subjective uncertainty in the choice of observed 'data', and their weighting, from the published contour maps was a much larger source of error than that associated with the fit to any particular data set.)

The parameters and orbital elements that correspond to the closest fitting jets are given in Table 2 and displayed superimposed on the 2.7- and 1.4-GHz maps taken from Burch (1977) in Figs 2 and 3. It can be seen that the fitted jet follows the observed contours fairly well, reproducing the sharp bends at A and B, and their more gradual southern counterparts at C and D. The indentation at E is not well imitated; neither are the bends in the outermost parts of the source.

3.3 SENSITIVITY OF FIT TO CHANGES IN THE PARAMETERS

As the best fit is obtained when both the jet and the orbital plane make small angles ($\sim 10°$) with the direction to the observer, small changes in i or ϕ generate large changes in the projected shape of the jet; and though i and ϕ can therefore be found with some precision, the derived value of m is fairly uncertain and the mass to light ratios are probably good to no better than 50 per cent.

Table 2. Parameters and orbital elements for the jet trajectory displayed in Figs 2 and 3.

mass of NGC 383 ($M_\odot$)	m_1	1.2×10^{12}
mass of NGC 382 ($M_\odot$)	m_2	3.1×10^{11}
perigalacticon separation (kpc)	$p/(1+e)$	53
eccentricity	e	1.0
longitude perigalacticon	ω	176°
orbital inclination	i	98°
present true anomaly	ζ	89°
north jet speed at infinity (km/s)	$u_{N\infty}$	420
south jet speed at infinity (km/s)	$uS\infty$	520
north jet polar angle	θ	72°
north jet azimuth	ϕ	272°
core size for NGC 383 (kpc)	c_1	11
core size for NGC 382 (kpc)	c_2	37

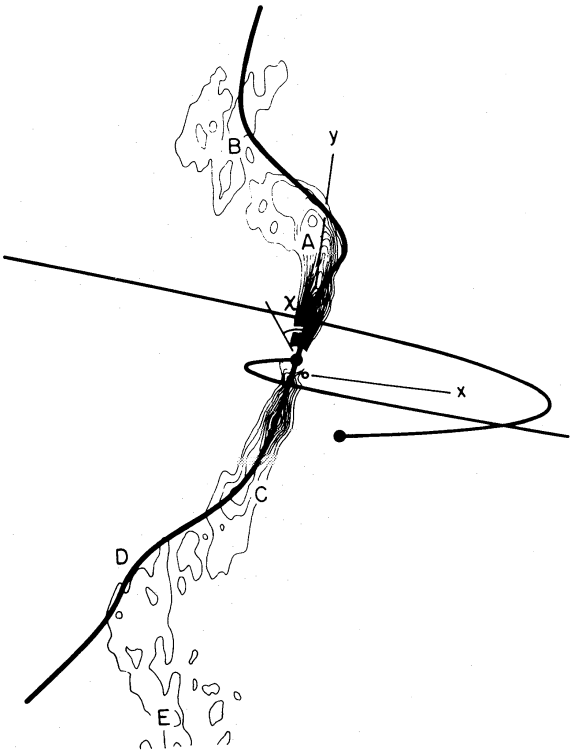

Figure 2. Jet trajectory for orbital parameters given in Table 2 superimposed on the 2.7-GHz map taken from Burch (1977).

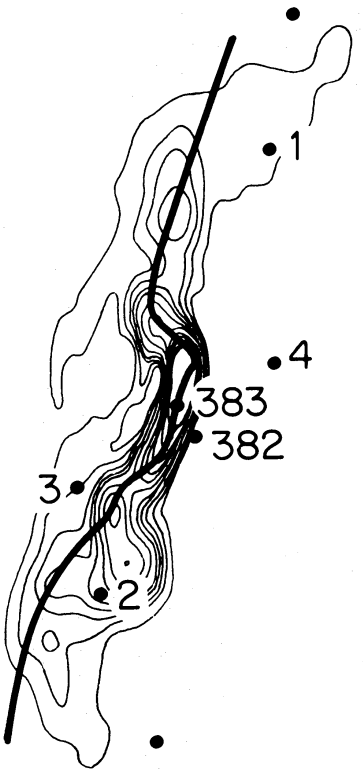

Figure 3. Jet trajectory shown in Fig. 2 superimposed on the 1.4-GHz map taken from Burch (1977). Nearby galaxies are also shown. Galaxy 1 is NGC 380 and galaxy 2 is NGC 386.

The influence of the other parameters on the apparent jet shape can be summarized as follows. The distance between NGC 383 and point A depends on u_N and ϕ; the uncertainty in ϕ is $\sim \pm 15°$. The velocity u_N must be large enough for the jet to climb out of NGC 383's potential well, the depth of which is determined by the core radius c_1. The more relevant quantity is the terminal velocity $u_{N\infty}$ achieved by the jet in the absence of a dynamical interaction with NGC 382. This is given by

$$u_{N\infty} = (u_N^2 - 2G\,m_1/c_1)^{1/2}. \tag{8}$$

The value of $u_{N\infty}$ is controlled mainly by the angle the jet makes with **n**, which is poorly determined. $u_{N\infty}$ is fixed to no better than a factor of 2 but its projection onto the sky is rather better determined.

The distance A–B depends rather sensitively on m_1/m_2; the uncertainty in the mass ratio is estimated to be about 30 per cent. The angle between AB and the northern continuation of the jet depends somewhat on $u_{N\infty}$, but not very sensitively; mostly, this angle is influenced by the eccentricity of the orbit, in the sense that a decrease in e makes the angle more acute (so that the jet bends to the north-east) and an increase makes it closer to a right angle. It was found that $e < 0.8$ (elliptical orbits) gave a markedly inferior fit. Eccentricities $\gtrsim 1.6$ were found to generate jets with bend angles that are far more obtuse than is observed. The best value appears to be $e \sim 1$, but with considerable uncertainty (about +0.3, −0.2).

The same considerations hold, *mutatis mutandis*, for the southern jet. There is one additional feature here, namely the location and size of the wiggle at E, attributed to the gravitational attraction of NGC 382. We found that its location could be somewhat influenced by means of $u_{S\infty}$, but the choice of this parameter is restricted by the required fit south of point E. The most important parameter turned out to be, of course, the angle θ, because it primarily determines the distance of closest approach between NGC 382 and the jet. The uncertainty in θ is estimated at about 10 per cent. Despite all our efforts, we did not manage to make the jet fit at all well at E, not even by sacrificing the fit of the northern jet.

Lastly, there is the problem of the model potential well and the core radii. Instead of the potential used above (equation 3), we also tried $\Phi_i = -Gm_i(|\mathbf{r}(t') - \mathbf{R}_i(t')|^4 + c_i^4)^{-1/4}$, which did not give noticeably different results. The influence of NGC 383's core size c_1 turned out to be small; any value $0.1 \leqslant c_1 \leqslant 1$ gave acceptable results. However, the value of c_2 appeared to be very important: for all $c_2 < 0.4$, corresponding to ~ 35 kpc, the impulse imparted to the southern jet at E and to the northern jet at A became so large as to destroy the fit.

4 Discussion

Before we describe some possible implications of our model for 3C 31, we must first discuss the assumptions on which it is based.

4.1 ASSUMPTIONS ABOUT THE DYNAMICS

NGC 383 is a member of a small group (Arp 331) located on the outskirts of the cluster Abell 262 (Moss & Dickens 1977). A high-contrast print of the area around NGC 383 from a plate taken at the Kitt Peak National Observatory by Dr H. C. Arp is shown in Plate 1. Of the galaxies around NGC 383/382, redshifts are only known for NGC 380 ($\Delta V_r = |V_r - V_0| = 610$ km s, with $V_0 = 4942$ km s the barycentric velocity of the NGC 383/382 system) and NGC 386 ($\Delta V_r = 600$ km s). The two smaller galaxies (designated 3, 4 in Fig. 3) are not as yet known to be associated with NGC 383.

How likely are these neighbouring galaxies to perturb the orbit in NGC 383 from its assumed Keplerian form? We can best quantify this by introducing a parameter

$$k = \sqrt{(2/3)}\, Gm_g\, [d\sqrt{(3/2)}]^{-2} \left\{ \frac{2d\sqrt{(3/2)}}{\Delta V_r \sqrt{3}} \right\} \left\{ 2\, \frac{m_2}{m} \left(\frac{Gm}{p} \right)^{1/2} \right\}^{-1} \tag{9}$$

which is a very rough estimate of the ratio of the velocity kick imparted to NGC 383 by a galaxy with mass m_g at an assumed distance of $\sqrt{3}/2d$ (where d is its projected distance and $\Delta V_r \sqrt{3}$ its relative space velocity), to the kick imparted by NGC 382.

Weighing the galaxies by their apparent magnitudes, we find that $k(380) \sim 0.4$, $k(386) \sim 0.1$; if the radial velocities of galaxies 3 and 4 are more than about 200 km/s different from that of NGC 383, then their k values are $\lesssim 0.3$. Of course it is impossible to exclude a recent encounter with one of these galaxies, but this criterion tells us that it is not at all unlikely that their gravitational influences can be ignored (at the 20 per cent level). Similar remarks apply to the gravitational influence of these companion galaxies on the jet, although, as both NGC 380 and NGC 386 lie along the projected jet, the probability of interaction is somewhat increased. (In fact we might attribute the kink at E, which has not been reproduced by our model, to just such an interaction with NGC 386.) With the derived perigalacticon separation of about 50 kpc, it can be seen that the tidal effect of NGC 383 or NGC 382 is very small, within ~ 20 kpc, and there should be no significant dynamical heating of the galaxies at the expense of the orbital energy. If, however, the projection effect was not as large as we are arguing and the perigalacticon separation was $\lesssim$ 25 kpc, then a noticeable distortion of the outermost isophotes should have been easily observed. This also implies that the deviations of the galaxies' orbit from Keplerian form are not important.

4.2 INNER JET

We must next examine our assumption that the jet moves ballistically and under the influence of gravity only, and that the effect of the surrounding medium can be ignored. At a reference deprojected distance of 75 kpc from NGC 383 along the northern jet, we find that the width d of the jet is about 5 kpc, implying a lower bound on the Mach number of the flow $M \gtrsim 15$ if the jet is out of pressure equilibrium with its surroundings, since the jet will then expand laterally at the internal sound speed (*cf.* Readhead, Cohen & Blandford 1978). If we make the standard equipartition assumption and allow for projection effects, then the minimum energy density at this distance is $\sim 10^{-14}\,\mathrm{J\,m^{-3}}$. Using the best-fitting jet speed of ~ 450 km/s, this gives a lower limit to the total power L in the supersonic jet of about 3×10^{34} W, a factor of ~ 3 greater than the integrated power of the whole source (predominantly inverse Compton scattering of the microwave background). The corresponding mass flux in the jet is $\dot{M} \sim 6 M_\odot$/yr.

If the jet is in pressure equilibrium with its surroundings, then pressure gradients will cause our ballistic model to be modified unless the Mach number is large. However, we note that the inferred density ($\sim 10^{-25}\,\mathrm{g\,cm^{-3}}$) and field strength ($\sim 3\,\mu$G) are not too dissimilar from those of the interstellar medium and so most of the mass may be clumped into clouds. If the jet forms a 'two-phase medium' of cool filaments imbedded in a hot tenuous gas, the inertia of the jet is due to the filaments, while pressure differences across the jet boundaries are felt by the hot component only. In this case, the assumption of ballistic motion will be justified if the radio-emitting regions are coupled to the filaments by magnetic fields.

Using these parameters, we can estimate the expected additional curvature in the jet due to motion of its surface with a speed $\sim (m_2/m)(Gm/p)^{1/2}$ through the surrounding medium, which has a density ρ. If the jet has a diameter d, the force per unit length acting on it is

$\sim \rho d(Gm_2^2/mp)$. Equating this to the centrifugal force gives an estimate of $(\rho d/\dot{M}u_\infty)$ (Gm_2^2/mp) for the additional curvature. As long as $\rho \lesssim 10^{-24}\,\mathrm{kg\,m^{-3}}$, the motion of the jet should not be affected by the surrounding medium even at a distance of 200 kpc from the galaxy. The situation is quite different in the central regions of X-ray emitting rich clusters of galaxies where most of the prominent radio trails are found. Here the velocities are several thousand km/s and the densities are in excess of $10^{-24}\,\mathrm{kg\,m^{-3}}$ (e.g. Jaffe & Perola 1973).

The neglect of pressure forces may be invalid in the vicinity of NGC 382 and NGC 383. We have found that it is only possible to fit the jet if the core radius for NGC 382 exceeds 35 kpc, at least three times the apparent size of the galaxy. With the orbit shown in Fig. 2, the southern jet passes within ~35 kpc of NGC 382 at the time when $\zeta \sim -90°$, and the northern jet passes a comparable distance away when $\zeta \sim 90°$. The relative velocity between the jet and the galaxy is ~250 km/s. In order to reproduce the bend at A, we have found that it is imperative to soften the effect of NGC 382's gravity. (It is a curious fact that if the attraction of NGC 382 is completely ignored then it is possible to obtain a fit that very accurately reproduces the contours in Fig. 2 with the exception of the kink at E. The orbital elements so obtained are quite similar to those given in Table 2.) This softening may be achieved if most of the mass in the galaxy is contained in an extended subluminous halo, or alternatively could be caused by gradients of gas pressure in a dense atmosphere ($\rho \gtrsim 10^{-24}\,\mathrm{kg\,m^{-3}}$) centred on NGC 382. An additional benefit of the latter assumption is that it can explain the large kink at E in the southern jet. A consideration of the interaction geometry (Fig. 1) shows that the jet would be brushed aside in the direction observed and the increased radio brightness near E might be attributed to this interaction.

There is another potential problem with the dynamics of a free supersonic jet. If the velocity gradient parallel to the jet is too large, then pressure gradients will be unable to resist the compression of the gas, and shocks may be expected to form. If the source of the jet does not accelerate, then this simply imposes a constraint on the amplitude of long timescale fluctuations in the jet velocity u for, if a very strong shock can form, the consequent pressure jump in the material across the shock would probably lead to transverse expansion, destroying the integrity of the jet unless the shock is radiative. When the source is being accelerated, the gas dynamics becomes more complicated. A rough criterion for the validity of our 'ballistic' assumptions can be shown to be $M \lesssim u^2/dg$ where g is the acceleration of the source (assumed never to be parallel to the jet). This is automatically satisfied provided that the Mach number does not significantly exceed the minimum value defined by the expansion angle of the jet.

From the estimated jet luminosity, velocity and field strength, we can derive a value for the rotation measure across the jet. At our reference distance of 75 kpc in a free jet, this turns out to be $\sim 2000\,\mathrm{rad\,m^{-2}}$ if the density of plasma in the jet is uniform and the field is ordered. For uniform expansion in the jet, this scales proportional to r^{-2}. We expect that the magnetic field component perpendicular to the velocity predominates and decays proportional to r^{-1}. Therefore, in a homogeneous jet we have a large rotation measure, and hence strong depolarization; the polarization vectors should (after subtraction of the Faraday rotation) roughly map out the velocity field. As the jet points within ~10° to the line of sight, the polarization should be low, but preferentially at right angles to the observed jet between the points A and B in Fig. 2. At larger distances the polarization vector should be parallel to the jet. If the jet is in pressure equilibrium with its surroundings, however, a parallel magnetic field may be produced by shear flow at the jet boundary.

Preliminary analysis of polarization observations (Burch, private communication) indicates that the rotation measure is much smaller than $2000\,\mathrm{rad\,m^{-2}}$, and so in order to transport enough mass, to justify our ballistic assumption, the jet must be inhomogeneous, as discussed above.

4.3 OUTER JET

Large-scale curvature is also observed in the outer jet and this is not at all well reproduced by our dynamical model. In fact, it would only be possible to obtain it by an interaction with NGC 382 if the orbit were bound with an eccentricity $e \lesssim 0.3$, and this would fail to reproduce the inner parts of the jet with any precision. It seems far more likely that this outer structure be attributed to one of the following:

(1) Earlier, independent dynamical encounters of NGC 383. On the basis of computer simulations of the dynamics of small groups (Rose 1977), we estimate a mean 'collision time' $\sim 10^9$ yr, adequate to account for the observations.

(2) Gas dynamical interaction between the radio source and large-scale motions in the surrounding medium (*cf.* Burch 1977).

(3) Buoyant motion in the average gravitational field of the Pisces group (Moss & Dickens 1977; *cf.* Cowie & McKee 1975).

There is evidence of the need for re-energizing the relativistic electrons in the outer parts of 3C 31 (Burch 1977). We note that differential motion in the jet induced by acceleration of the NGC 383 may be one way of bringing this about. It is not clear how far the contiguous radio emission extends in 3C 31 but, if the jet is to travel out to a projected distance of 400 kpc and $u_\perp$ is constant at ~ 80 km/s, the age of the source is $\sim 5 \times 10^9$ yr.

4.4 VALIDITY OF THE DYNAMICAL MODEL

We think that the above dynamical interpretation of 3C 31 is reasonable, because the following key features are reproduced by our orbit (without its having been constrained to do so):

(1) The large ratio (~ 3) of the distance of closest approach of the galaxies to their present projected separation, as indicated by the apparent absence of tidal effects.

(2) A mass ratio, roughly proportional to the light ratio on the basis of the estimated magnitudes of the galaxies.

(3) Velocities for the northern and southern jets that are large enough to ensure escape from NGC 383 with a central velocity not greatly in excess of the asymptotic velocity. If the jet made a substantially larger angle with the line of sight, this would not be the case.

(4) An eccentricity ~ 1 implying a small relative velocity at infinity.

(5) A derived mean mass of V-band light ratio (Table 1) of ~ 11 solar units, which is entirely consistent with statistical estimates based on double galaxy observations (Turner 1976), virial estimates for small groups (Rose 1977; Gott & Turner 1977), a 'velocity dispersion' determination for the outer parts of M87 (Sargent *et al.* 1978), and dynamical modelling of more dramatic galaxy encounters (Toomre & Toomre 1972). Of course, this mass to light ratio implicitly depends on the published radial velocities, the estimated magnitudes of the galaxies, and the assumed value of the Hubble parameter ($50\,\mathrm{km\,s^{-1}\,Mpc^{-1}}$). Its value may be altered by a redetermination of the first two quantities, but in the case of 3C 31 it is the quality of the fit that will ultimately determine the accuracy of the measurement.

However, this interpretation does not carry complete conviction because, as we have discussed, the fit is not especially good, the potential of NGC 382 must be artificially softened, the influence of other nearby galaxies, especially NGC 380, must be neglected and the neglect of gas-dynamical forces cannot be completely justified.

4.5 APPLICATION TO OTHER SOURCES

Several other low-power sources have been shown to display radio jets and some of these show pronounced wiggles. Examples include B 0844 + 31, 3C 129, 3C 310 (van Breugel & Miley 1977), 1200 + 519 (Miley & Harris 1977) and 3C 449 (Högbom & Carlsson 1974). The latter three are particularly good candidates, as in each case the galaxy associated with the radio source has a close companion, known to be interacting in the case of 3C 449. However, the other examples do not have obvious companions. It would also be of interest to obtain high-sensitivity maps of extended radio sources associated with known double galaxies (Stocke, Tifft & Kaftan-Kassim 1978).

We have derived jet speeds of ~ 500 km/s for 3C 31. This value is somewhat lower than that inferred for high-power sources like Cygnus A (Hargrave & Ryle 1974). Nevertheless, as the total radio power of 3C 31 is ~ 10^{-4} that of Cygnus A, it is not unreasonable that its jet speed be much lower.

5 Conclusions

On the basis of our dynamical model for 3C 31 we conclude that the innermost radio contours can be adequately reproduced by setting the galaxies NGC 383/382 in an unbound orbit with parameters given in Table 2, provided that the gravitation attraction of NGC 382 is softened within ~ 35 kpc. This implies masses of ~ 10^{12} and ~ $3 \times 10^{11} M_{\odot}$, respectively for NGC 383 and 382, a corresponding mean mass to light ratio ~ 11 in V magnitude solar units, and jet speeds of ~ 500 km/s. This method of mass determination may be applicable to other radio trails such as 3C 449.

Acknowledgments

We are indebted to H. C. Arp for discussion and for supplying the plate. We also thank S. F. Burch, C. F. McKee and A. C. S. Readhead for helpful comments. This work was supported in part by the National Science Foundation grants AST76-20375 and AST76-80801 A01.

References

Arp, H. C., 1966. *Atlas of peculiar galaxies,* California Institute of Technology.
Bridle, A. H., David, M. M., Meloy, D. A., Fomalont, E. B., Strom, R. G. & Willis, A. G., 1976. *Nature,* **262,** 179.
Burch, S. F., 1977. *Mon. Not. R. astr. Soc.,* **181,** 599.
Byrd, G. G. & Valtonen, M. J., 1978. *Astrophys. J.,* **221,** 481.
Cowie, L. L. & McKee, C. F., 1975. *Astr. Astrophys.,* **43,** 337.
Gott, J. R. III & Turner, E. L., 1977. *Astrophys. J.,* **213,** 309.
Hargrave, P. J. & Ryle, M., 1974. *Mon. Not. R. astr. Soc.,* **166,** 305.
Högbom, J. A. & Carlsson, I., 1974. *Astr. Astrophys.,* **34,** 341.
Humason, M. C., Mayall, N. U. & Sandage, A. R., 1956. *Astr. J.,* **61,** 97.
Jaffe, W. J. & Perola, G. C., 1973. *Astr. Astrophys.,* **26,** 423.
Karachentsev, I. D., 1972. *Comm. Spec. Astrophys. Obs. USSR,* **7,** 1.
Miley, G. K. & Harris, D. E., 1977. *Astr. Astrophys.,* **61,** L23.
Moss, C. & Dickens, R. J., 1977. *Mon. Not. R. astr. Soc.,* **178,** 701.
Readhead, A. C. S., Cohen, M. H. & Blandford, R. D., 1978. *Nature,* **272,** 131.
Rose, J. A., 1977. *Unpublished thesis,* Yale University.
Sargent, W. L. W., Young, P. J., Boksenberg, A., Shortridge, K., Lynds, C. R. & Hartwick, F. D. A., 1978. *Astrophys. J.,* **221,** 731.

Stocke, J. T., Tifft, W. G. & Kaftan-Kassim, M. A., 1978. *Astr. J.*, in press.
Toomre, A. & Toomre, J., 1972. *Astrophys. J.*, **178**, 623.
Turland, B. D., 1975. *Mon. Not. R. astr. Soc.*, **172**, 181.
Turner, E. L., 1976. *Astrophys. J.*, **208**, 304.
van Breugel, W. J. N. & Miley, G. K., 1977. *Nature*, **265**, 315.
Waggett, P. C., Warner, P. J. & Baldwin, J. E., 1977. *Mon. Not. R. astr. Soc.*, **181**, 465.
Wellington, K. J., Miley, G. K. & van der Laan, H., 1973. *Nature*, **244**, 502.